

Gravity image generation over the Indian subcontinent using NGRI/EGM96 and ERS-1 altimeter data

T. J. Majumdar^{†,*}, K. K. Mohanty[†], D. C. Mishra^{**} and K. Arora^{**}

[†]Marine and Water Resources Division, Remote Sensing Applications Area, Space Applications Centre (ISRO), Ahmedabad 380 015, India

^{**}National Geophysical Research Institute, Uppal Road, Hyderabad 500 007, India

A new technique for merging of land gravity using NGRI/EGM96 and ocean gravity using mainly ERS-1 altimeter-derived gravity data has been described. Methods for generation of residual/prospecting geoids and free-air gravity anomaly over Indian oceans surrounding Indian land mass using satellite altimeter data have already been developed. Recently Earth Gravity Model (EGM) 1996 data over the Indian land mass were available through Internet. It is, therefore, emphasized that a joint gravity image over the whole subcontinent, which includes land and ocean, will be of paramount importance for further studies in geophysical exploration/earth science studies in this region. Also, comparison of EGM96 data over certain profiles with satellite-derived information has shown the efficacy of the Satellite Gravity Method. Maps of gravity anomaly generated over the Indian subcontinent using ERS-1 altimeter/EGM96 data are presented along with their interpretation. A number of known megastructures over the study area, e.g. Bombay High, Saurashtra Platform, 90° East ridge over the oceans, etc. and Himalayan Thrust Belt, Narmada–Son Lineament, Saurashtra Block, Dharwar Block and other major tectonic/structural features and their subsequent extension inside the sea could be successfully interpreted from these maps. Similar attempts have also been made with National Geophysical Research Institute (NGRI) generated gravity over land and altimetric/EGM generated gravity over oceans.

GRAVITY field models are being used for different applications which include orbit determination of spacecraft, a variety of geophysical investigation/exploration, oceanographic investigations using satellite altimetry, including offshore exploration for petroleum. Surface gravity data provide a more direct measurement of the gravity field, but acquiring data uniformly over the earth has always been difficult. Because the sea surface largely conforms to the geoid, satellite altimetry provides precise measurements of the marine gravity field, provided that proper corrections are made to altimeter

data due to atmospheric parameters, instrumental bias, satellite tracking, dynamic topography and other relevant errors¹.

Regional gravity anomaly maps provide valuable information on the subsurface density distribution, major tectonic and structural lineaments, geodynamic aspects of a plate margin and structure of the crust and lithosphere². The rapid assessment of offshore sedimentary basins has been the need of the present-day geophysical exploration³, for which satellite altimetry has emerged as a powerful reconnaissance tool in recent years^{4–7}. The basic concept of the technique is that the surface of any water body, in the absence of external forces, forms an equipotential surface. The sea surface height measured by satellite altimeter when corrected for atmospheric propagation delays and dynamic oceanic variabilities, conforms to the equipotential surface known as the geoid (Figures 1 and 2). The geoid contains information regarding mass distribution inside the entire earth, including that due to variations in sea bottom topography, which is used to compute residual/prospecting geoids – hypothetical surfaces related to the mass distribution in various lithospheric zones.

Brennecke and Lelgemann⁸ have used Seasat altimeter data for exploring offshore geological structures in the Atlantic Ocean. Haxby *et al.*⁹ have generated digital images from the combined oceanic and continental data sets and have specified their usages in tectonic studies. Rapp¹⁰ has used spherical harmonic coefficient expansions up to degree and order 30 and above for determination of gravity anomaly. Craig and Sandwell¹¹ have identified a number of seamounts in the transition zone off the Indian coast. A tentative correlation has been established between geoid and bathymetry in the short wavelength region (0–300 km) by McKenzie and Bowin¹². Lundgren and Nordin⁴ and Srivastava *et al.*¹³ have developed a brief methodology for offshore structure delineation using altimeter data.

The technique called ‘Satellite Gravity Method’, originally developed by Petrosan Inc, Sweden, for generation of residual and prospecting geoids and the related gravity anomalies using satellite altimeter data has been attempted at Space Applications Centre

*For correspondence. (e-mail: rajesh-sathya@hotmail.com)

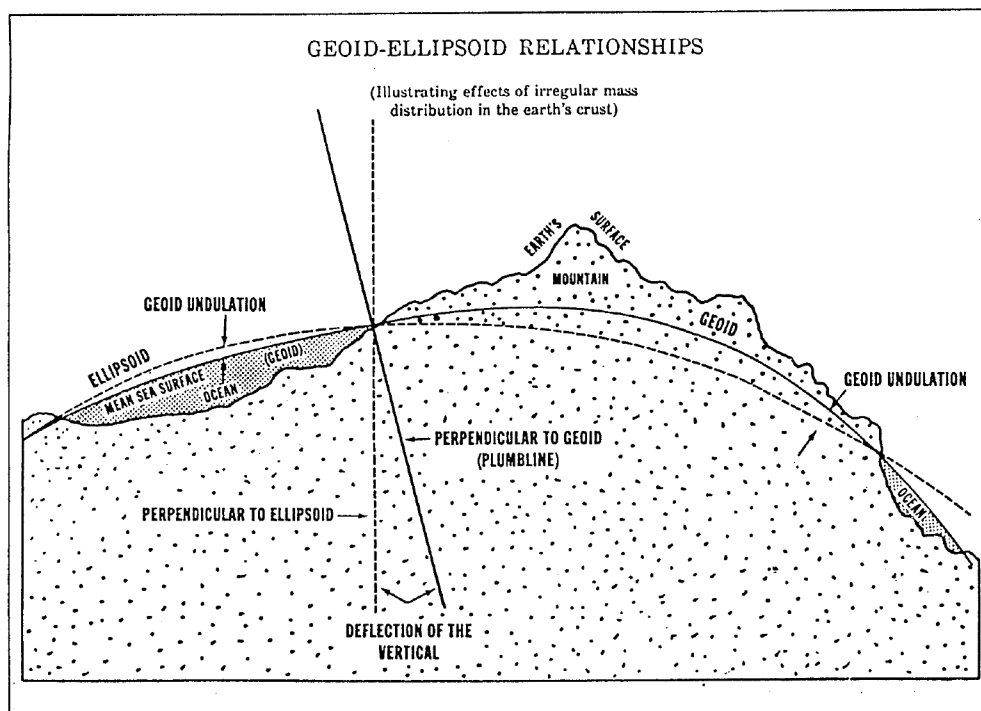


Figure 1. Geoid-ellipsoid relationship (after ref. 33).

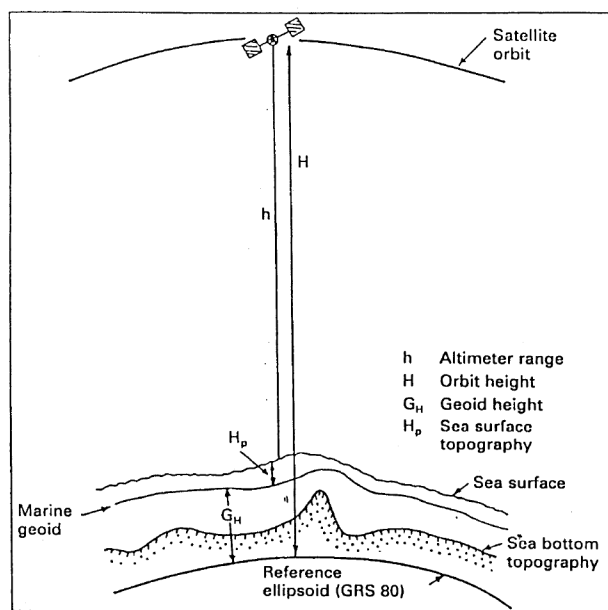


Figure 2. Basic concepts of satellite altimetry (after ref. 34).

(ISRO), Ahmedabad in collaboration with K. D. Malaviya Institute of Petroleum Exploration (ONGC), Dehra Dun and deliverables comparable to Petrosan, Inc. have been produced. One year ERS-1 altimeter data have been processed to generate prospecting geoid and gravity anomaly maps over the Indian Ocean. It was aspired to generate an image for the overall gravity es-

timation over the Indian subcontinent, including the land mass as well as the surrounding oceans, which would be extremely helpful to understand the tectonic processes that have taken place on earth in this region since the formation of the Gondwanaland. Also, it will be helpful in understanding the extension of different geological features from land to oceans and vice-versa, which has tremendous impact on the mineralogic/oil exploration processes in the land/ocean. However, generation of such a gravity image was difficult as the Satellite Gravity Method fails over land, as only the sea level under certain circumstances works as a natural gravimeter. However, gravity data from Earth Gravity Models (EGM96) are currently available from USA/NGDC via Internet, which are being used as an alternative to the paucity of data over land. The same has been procured and preprocessed to generate the free-air gravity data over land and then superimposed over the altimetric gravity over the oceans surrounding India, to generate a combined gravity image over the Indian subcontinent. Also, EGM96 data could be compared with satellite-derived (ERS-1) gravity over the Indian Ocean, in general, and in the case of certain profiles. National Geophysical Research Institute (NGRI), Hyderabad has collected ground gravity data over various grids over Indian land mass and has generated free-air and Bouguer gravity anomaly maps in 1:5 million scale, which have also been used in this study¹⁴.

The major objectives of the present study are (i) Generation of gravity anomaly image over Indian land mass

and its surrounding oceans using EGM96/NGRI gravity with ERS-1 altimeter-derived gravity data; (ii) Comparison of EGM96 derived gravity with altimeter-derived gravity over Indian oceans; (iii) Usage of gravity anomaly maps for mineral/hydrocarbon exploration *vis-à-vis* structural/tectonic interpretation.

EGM96 data over land have been obtained from Internet and preprocessed as given in Lemoine *et al.*¹⁵. NGRI gravity map data over land have been digitized and collated with altimeter-derived/EGM96 gravity data.

In the offshore study, we have used ERS-1 altimeter data (35/168-day repeat) over a period of one year⁶, in addition to EGM96 gravity data. ERS-1 altimeter tracks (168-day repeat) over the study area are shown in Figure 3. Details of ERS Geophysical Data Record (GDR) have been described elsewhere¹⁶. The study area has the latitude and longitude limits between 0–40°N and 55–105°E.

The geoid is a gravity equipotential surface approximating well to the mean sea surface over the ocean. The geoid contains more information regarding mass distribution inside the earth than the gravity alone, since gravity only represents the first derivative of the geopotential⁴. Sea surface height (SSH) observations, when averaged, minimize the effects due to dynamic sea surface topography, particularly in regions with seasonally varying currents such as the Arabian Sea. The contributions to the geoid can be broadly divided into three categories, (a) bathymetric contribution, (b) lithospheric contribution and (c) contribution due to deeper earth effects. For exploration of hydrocarbon-bearing structures, only the geoidal contribution due to the lithospheric zone is of significance. Bathymetry data along

the satellite track obtained from naval hydrographic charts have been used to model geoidal contribution due to bathymetry. The contributions due to deeper earth are removed using GEM 10B geopotential model expanded up to degree and order 50 (ref. 10). The geoidal undulation obtained after removing the contributions due to bathymetry and deeper earth is known as prospecting geoid (which corresponds to the mass distribution in the sedimentary layers), and is useful for delineation of offshore hydrocarbon-bearing structures^{4,17}.

The free-air gravity anomaly can be obtained from geoid using the relation¹⁸

$$F(\Delta g) = g_0 |k| F(N),$$

where $F(\Delta g)$ is the Fourier transform of free-air gravity anomaly, $F(N)$ is Fourier transform of geoid undulation and $|k|$ is one-dimensional wave number corresponding to wavelength λ .

Different components of the prospecting geoid and free-air gravity anomaly have been obtained using spectral analysis, through Fourier transform. Long, medium and short wavelength components extracted in this process can be related with different geological structures¹⁹. These components are interpreted jointly to derive a meaningful picture of the subsurface: (i) Long wavelength component (100–400 km) mainly reflects crustal events of regional proportions; (ii) Intermediate wavelength component (50–100 km) investigates shallower occurrences. These undulations can give information regarding development of regional depressions and tectonic trend; (iii) Short wavelength component (15–50 km) undulations are more closely related to basement topography and overlying sedimentary cover.

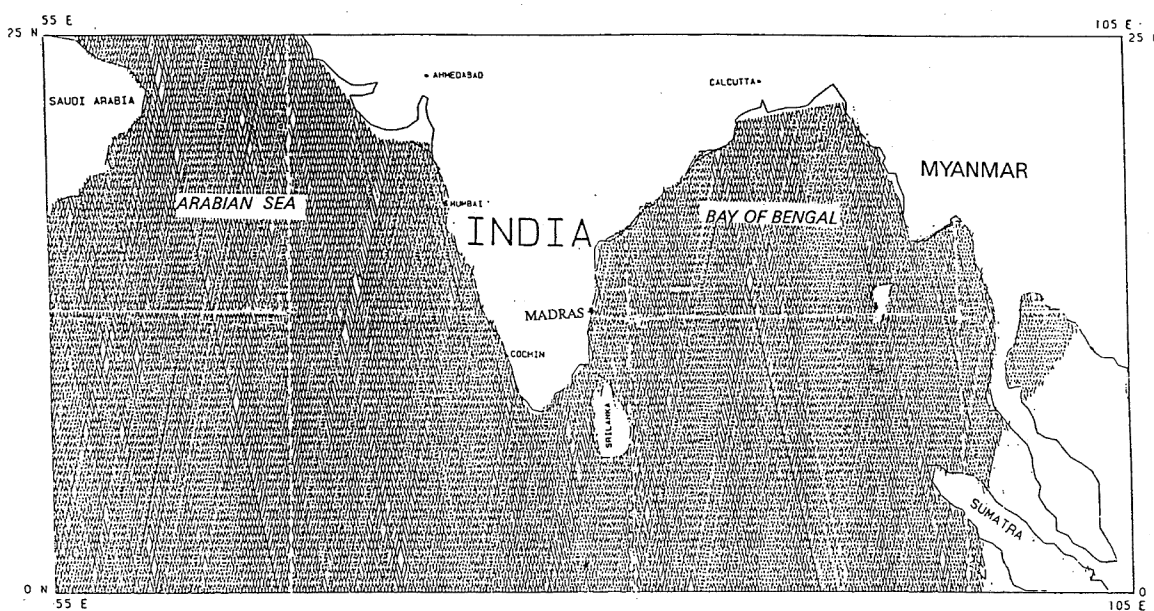


Figure 3. ERS-1 168-day repeat cycle tracks over the study area.

Figure 4 shows the data processing scheme used in offshore oil exploration.

The NASA Goddard Space Flight Center (GSFC), the National Imagery and Mapping Agency (NIMA), and the Ohio State University (OSU) have collaborated to develop an improved spherical harmonic model of the earth's gravitational potential to degree 360. The new model, Earth Gravitational Model 1996 (EGM96), incorporates improved surface gravity data, altimeter-derived gravity anomalies from ERS-1 and from Geosat Geodetic Mission (GM), extensive satellite tracking data as well as direct altimeter ranges from TOPEX/POSEIDON, ERS-1 and Geosat¹⁵.

The Bouguer gravity map brings out the following striking features^{14,20}: (i) Dominance of negative Bouguer anomalies over a major part of the subcontinent, reaching the maximum value of 380 mGal over the Himalayas; (ii) Belts of positive Bouguer anomalies are seen along the west coast between Thiruvananthapuram and Cochin, Mumbai and Ahmedabad. Positive anomaly trends characterize part of the east coast and the Shillong plateau; (iii) The trends of anomalies are parallel to the major structural trends, NNW-SSE Dharwar trend in south India, NE-SW Aravalli trend, ENE-WSW Satpura trend and the Himalayan trend²¹; (iv) Several gravity highs and lows may be identified. The sediments of the Vindhyan and Gondwana basins and the sedimentary tracts of the east coast and the intrusive granites of peninsular India are characterized by gravity lows. Gravity highs are observed over the Eastern Ghats, south-western Cuddapah basin, the Satpura and Aravalli ranges and the Shillong plateau.

These anomalies are possibly caused partly by deep seated features also²⁰. The latest version of the satellite-derived gravity field scans the deeper levels of the interior and has three major aspects: (a) A prominent ocean gravity low; (b) a gravity high in the Himalayas, and (c) a prominent NW-trending low to the south of the Himalayas.

The residual geoid and the free-air gravity anomaly images generated using ERS-1 altimeter data (168-day repeat) over oceans surrounding Indian peninsula are shown in Figures 5 and 6, respectively.

Figure 7 shows the bathymetric and tectonic features as observed in the residual geoid. It provides important information on structure of compensated lithosphere.

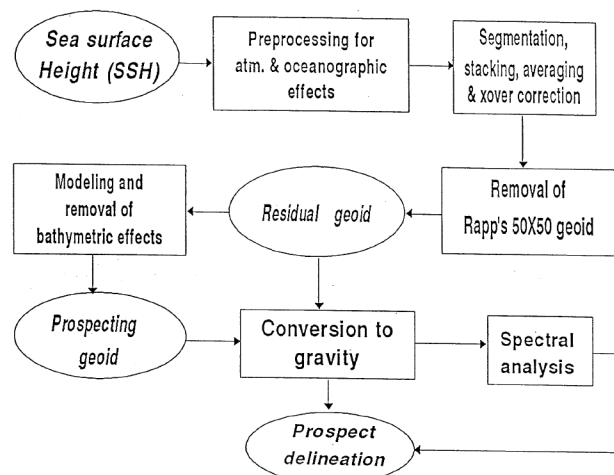


Figure 4. Data processing scheme used in offshore oil exploration.

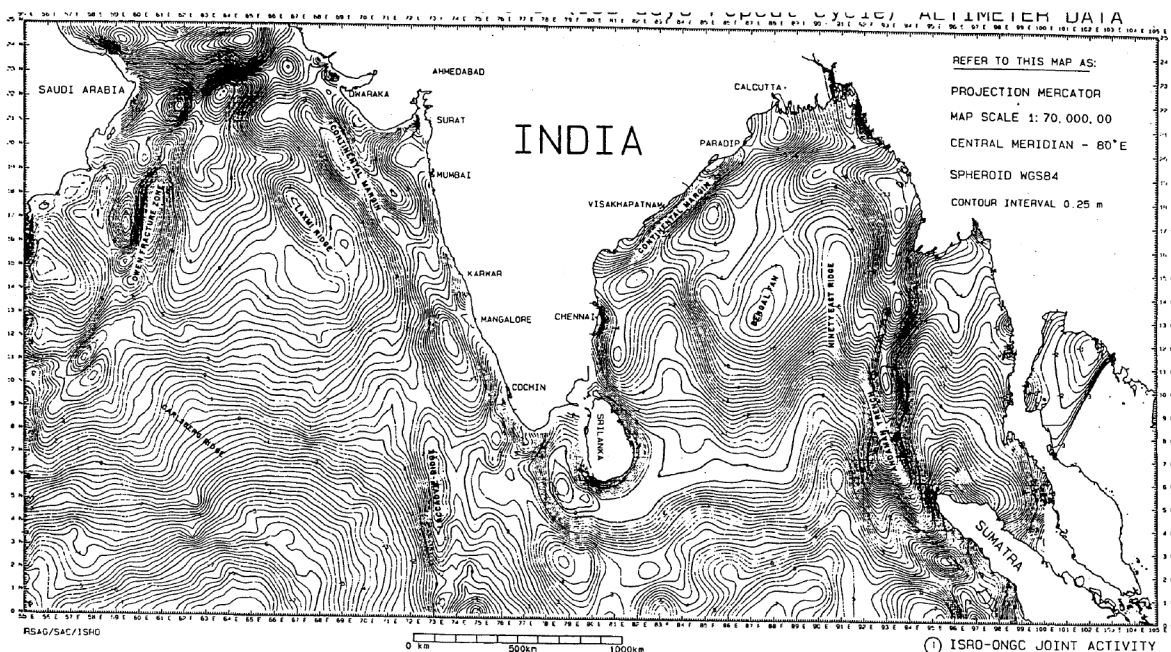


Figure 5. Residual geoid map over the study area from ERS-1 altimeter data.

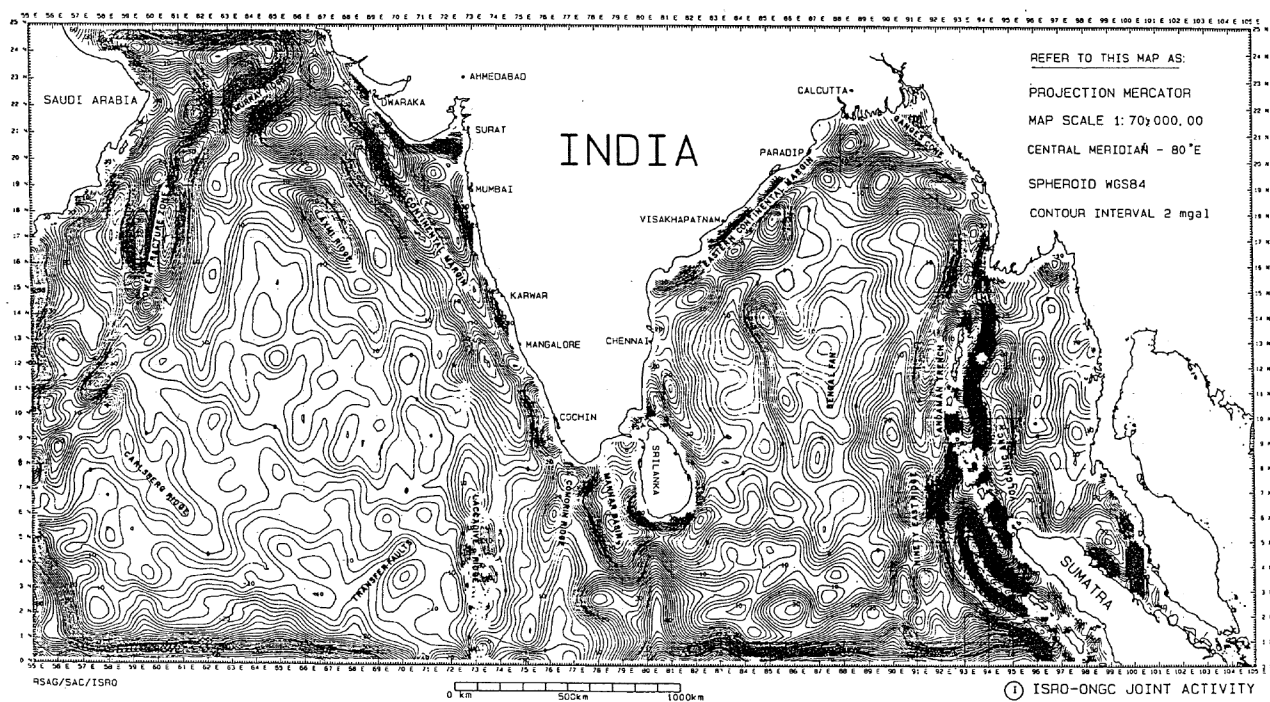


Figure 6. Free-air gravity anomaly map from ERS-1 altimeter data.

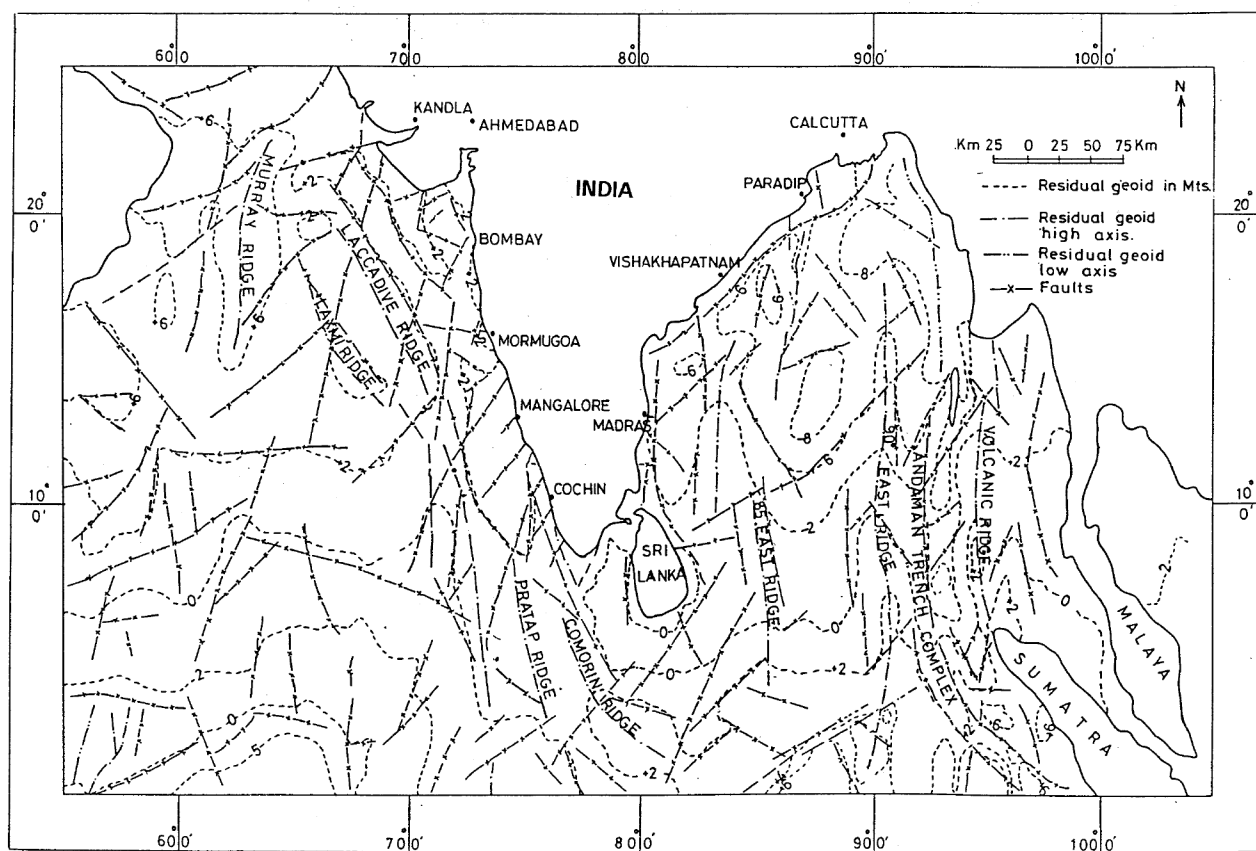


Figure 7. Bathymetric and tectonic features as observed in the residual geoid.

Geoid data, when combined with bathymetric knowledge, provide constraints on the earth's elastic response and thus on the cooling process of the oceanic lithosphere³⁵. Figure 5 shows the classical geoid patterns over the Indian offshore which match well with the findings of others¹⁰, with ranges varying between -56 and -106 m. The computed values range from -56 to -110 m, with the deepest low concentrated in the west of Sri Lanka. Major features which could be observed include Murray ridge, Laxmi ridge, Laccadive and Pratap ridges in the western offshore and 85° and 90° East Ridges, and Andaman trench complex in the eastern offshore region^{6,13,22}.

The negative geoid over a large part of the Indian Ocean indicates a major mass deficiency present in upper mantle which appears to be related to the formation of Indian Ocean as a result of break-up of Gondwanaland and separation of the Indian plate from Afro-Antarctica plate mosaic (and its northward flight) before collision with the Eurasian plate in the north²³.

Figure 6 shows the satellite-derived free-air gravity anomaly generated over the Indian offshore. The gravity anomaly values ranging from 40 mGal to -40 mGal and general trend of contours are NW-SE, except at the boundary zones near 6°N latitude. A series of gravity lows are observed near the Indian coast which may be related to low density recent sediments near the coast. Broad low observed in the contour map represents the Bengal fan sediments. The major trends observed are NE-SW, NW-SE, N-S and E-W which may represent the deformation pattern and the density distribution in the area. The Laccadive ridge and Ninety East ridge are relatively positive compared to the surroundings. To the east of 90° East ridge, a long belt of negative free-air anomaly follows the west coast of Sumatra (near 5°N, 95°E) which passes to the east of Andaman Islands and reaches up to Bengal basin near 24°N, 92°E. This represents the Andaman trench complex. The geoid and gravity signatures also clearly outline the limit of the continental shelf break in the eastern and western offshore regions.

Passive continental margin of western India is characterized by the presence of horst graben-like features, NW-SE trending regional faults, Laxmi ridge, Chagoes-Laccadive and Pratap ridge complexes and a basement high running approximately NW-SE off Mumbai (Figure 7). The geoid contour map over the western offshore also represents the transition zone between continental and oceanic crusts (Figures 6 and 7)¹³.

When compared with earlier maps²⁴ altimeter-derived free-air gravity anomaly over the Bay of Bengal reflects better results over distantly spaced ship-borne data. The chain of gravity lows near the coasts coincides with the shelf edge of the Indian continent.

The 85°E ridge is observed as a gravity low extending in N-S direction between 6° and 15°N (Figures 5-7).

Low gravity field at 85°E ridge is related to two-stage deformation of Bay of Bengal lithosphere, first when the ridge is emplaced over a young weak and thin oceanic lithosphere and secondly, when the lithosphere deformed in response to the sediment loading²⁵.

The 90°E ridge gravity signature is different from that of 85°E ridge. Here, the gravity anomaly at places rises to 30 mGal. The thickness of sediments over 90°E ridge is approximately 2.0 km²⁶. It is observed as a topographic high up to 10°N on bathymetry charts^{27,28}.

Gravity computed in the area under study has shown good resemblance with the major tectonic features. Laccadive ridge, Carlsberg ridge and Owen fracture zone are very well defined on the gravity map²⁵. Areas south of Bombay High represent deep continental shelf and Murud depression (Figure 6). Extent of Deccan trap in offshore has influenced the gravity signature in the Bombay High, and other surrounding blocks in the western offshore.

Figure 8 shows a profile of satellite (Geosat)-derived gravity across 90°E ridge at latitude 12°N in the eastern offshore. Continental slope as well as 85°E and 90°E ridges could be demarcated well along the profile⁵. In addition, almost all the structures have been demarcated in the Indian offshore in the residual geoid/free-air gravity maps as generated from ERS-1 35/168-day repeat altimeter data (Figures 5 and 6)^{23,29}.

Satellite altimeter data are highly cost-effective and require limited ship-borne surveys. Major geological features in the western and the eastern offshore regions have been demarcated using satellite altimeter-derived residual geoid and gravity anomaly. The present technique generates gravity anomaly beyond 200 m isobath, where ONGC has sparse geophysical data³. Some of the geological structures mapped in detail are the Bombay High, 90°E ridge, 85°E ridge, Andaman trench complex and Laxmi ridge (Figure 7)²³. Some of the potential sites identified for detailed investigation/validation are

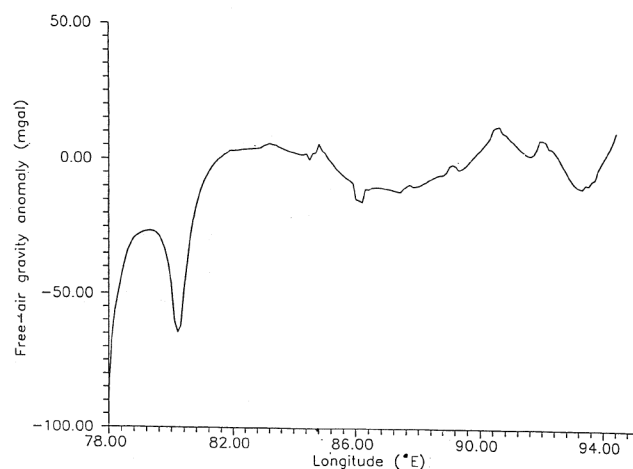


Figure 8. Profile of free-air gravity (from Geosat) across the Bay of Bengal (latitude: 12°N).

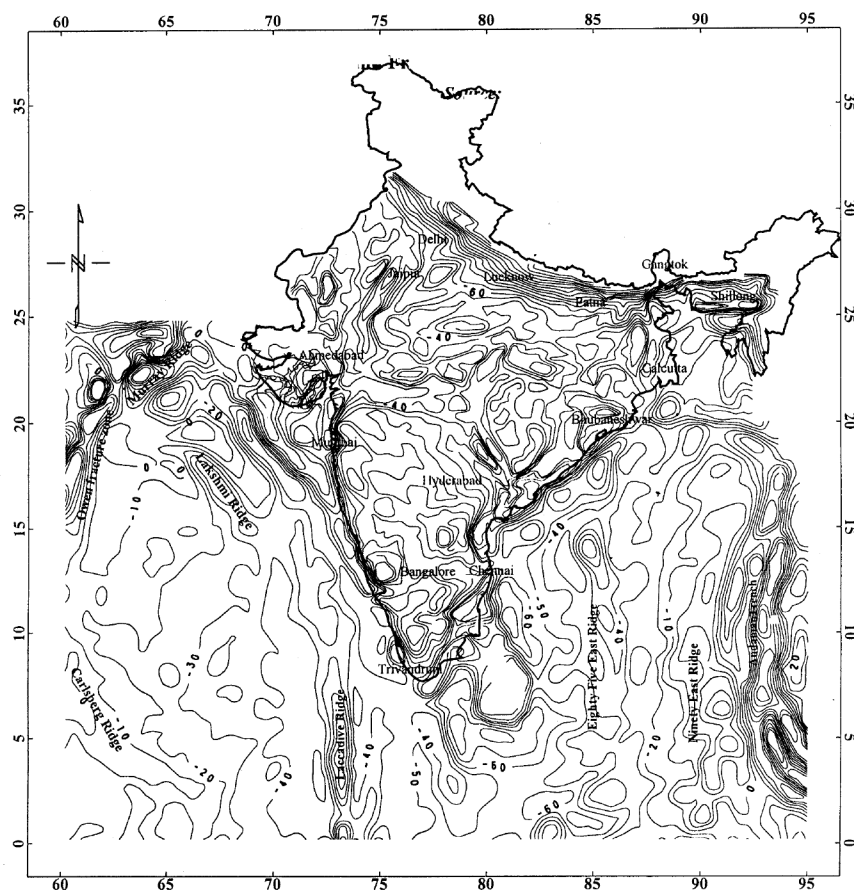


Figure 9. Bouguer anomaly over continent and free-air anomaly over adjoining oceans of India. (Source: NGRI, 1978 and GSB, 1990 for continent, EGM96 for oceanic region.)

west of Bombay High, north-east of Laxmi ridge, north of Laccadive ridge (Arabian Sea) and east of Palar basin (near Chennai coast), north of Krishna Delta in the off-shore, and Bengal Fan region (Bay of Bengal)²⁹.

The Bouguer anomaly map of India¹⁴ has also been digitized and the values interpolated at 10 km interval to prepare a composite gravity map of India. The gravity data for ocean are based on EGM96 data¹⁵. The satellite data provide free-air anomaly at $30' \times 30'$ grid for the Arabian Sea and the Bengal basin which are joined with the Bouguer anomaly of the Indian continent. The two are matched properly along the coast and the resulting gravity map is presented (Figure 9). As the Bouguer anomaly of the continents corresponds to the free-air anomaly of the oceans, it is justified to join the two data sets to prepare the composite map. Figure 9 depicts several gravity anomalies corresponding to important tectonic elements over the oceans and the continents. Some of the gravity anomalies of the oceans extend over the continents and vice versa, indicating the relationship between the continental and the oceanic structures. The most important among them are: (a) Extension of the

gravity 'high' of the continental shelf along the west coast of India over Saurashtra. This gravity high appears to correspond to the high density Deccan Trap rocks over the continental shelf of India. In fact, the gravity highs corresponding to Owen fracture zone and Murray ridge also extend over the continent which forms the plate boundary between the Indian and Arabian plates. (b) The other significant extension of the gravity anomaly from ocean to continent is that of 85° East ridge in the Bay of Bengal which extends over the Bengal basin and suggests the presence of high density volcanic rocks in this region. (c) The gravity highs of 90° East ridge spread along the continental shelf of West Bengal and Bangladesh and join with the gravity high of 85° East ridge. This suggests that the source of the two ridges in the Bay of Bengal may be same, which formed during the break-up of India from Antarctica during early-middle Cretaceous due to the Kerguelen hotspot.

In addition, NGRI and EGM96 terrestrial data have been superimposed over the ERS-1 altimeter-derived (35/168-day repeat) gravity data over the Indian Ocean, including the Arabian Sea and the Bay of Bengal.

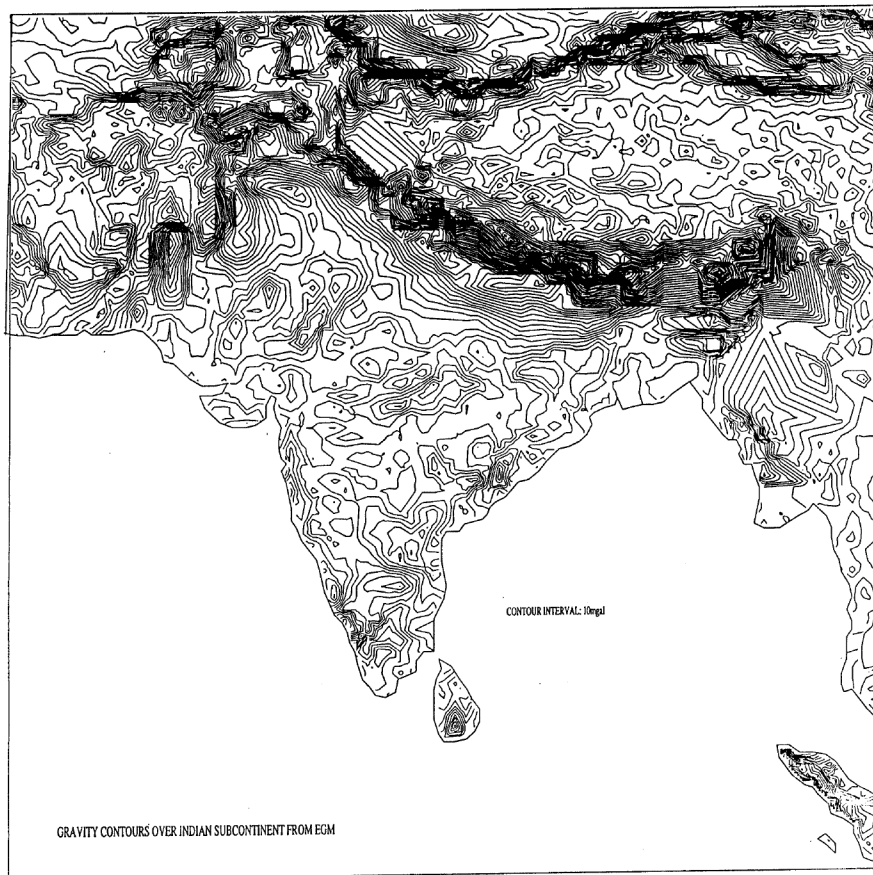


Figure 10 a. Free-air gravity generated over Indian subcontinent using EGM96 data.

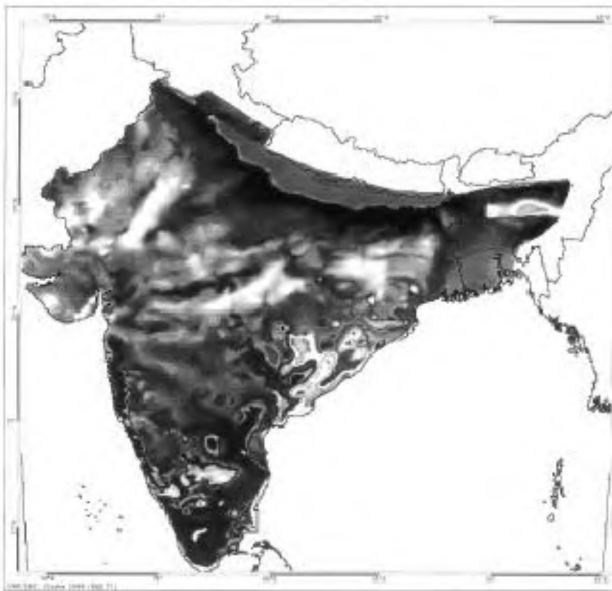


Figure 10 b. Free-air gravity generated over Indian subcontinent using NGRI gravity data.

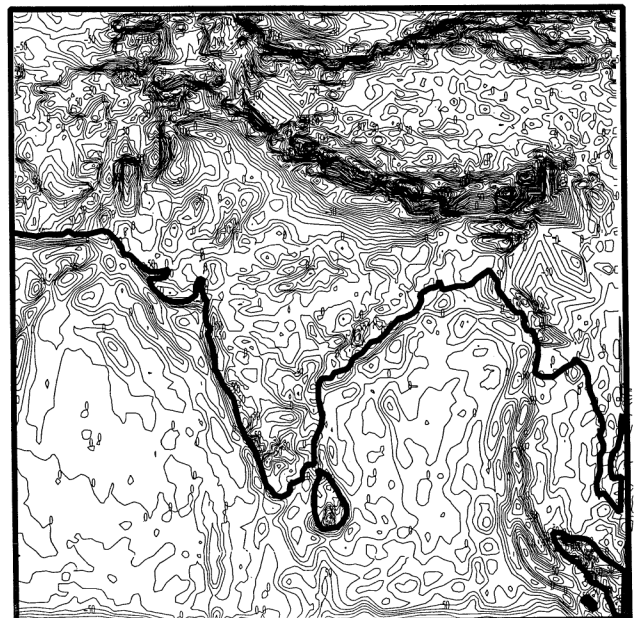


Figure 11 a. Total free-air gravity over Indian land mass and its surrounding oceans from EGM96 terrestrial data and ERS-1 altimeter data in the form of contours.

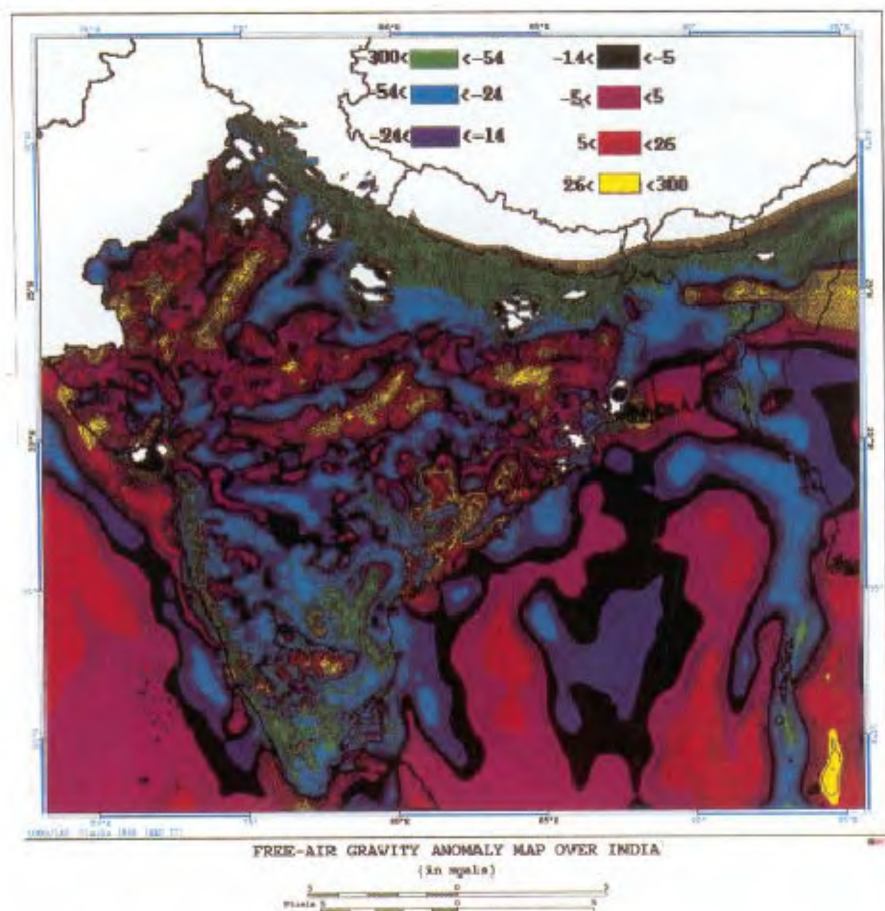


Figure 11 b. Total free-air gravity over Indian land mass and its surrounding oceans from EGM96 terrestrial data and ERS-1 altimeter data in the form of pseudo-colour.

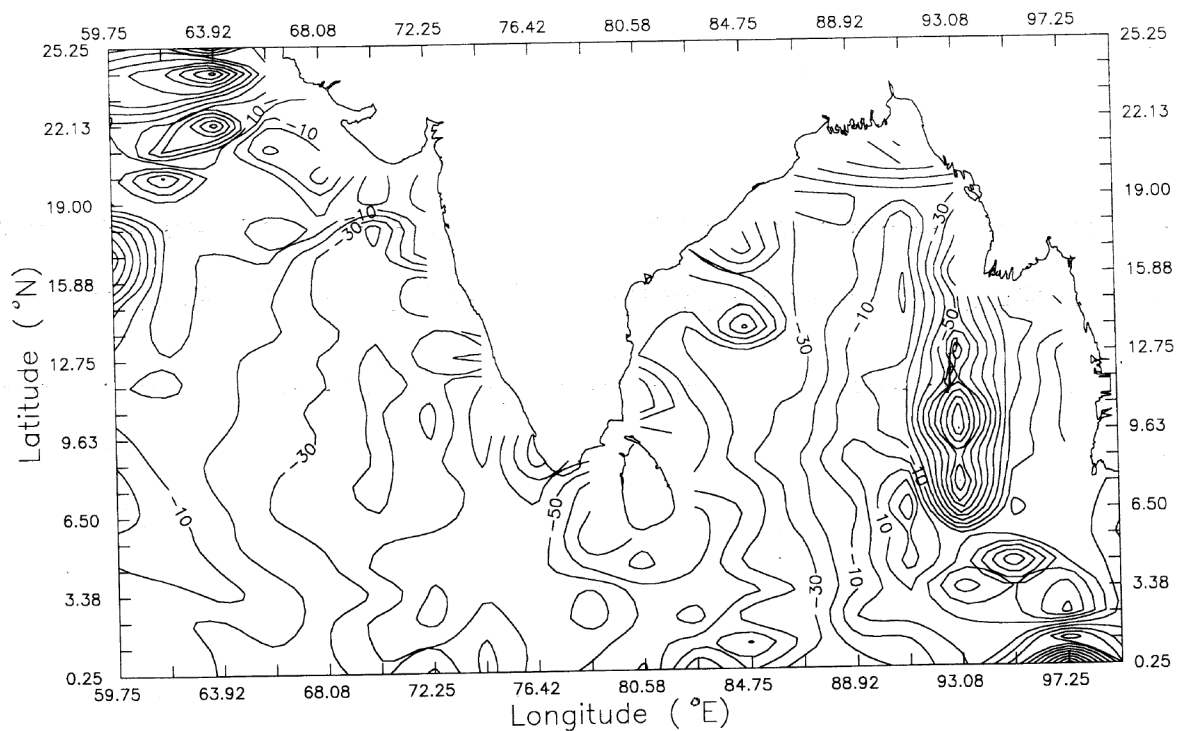


Figure 12. Free-air gravity over oceans surrounding Indian land mass as obtained from EGM96 data.

Figure 10 *a* and *b* shows the free-air gravity contours generated over the Indian subcontinent using EGM96 data and the gravity image generated over the same area using NGRI gravity data only. Figure 11 *a* and *b* shows the total gravity contours and colour image, respectively, generated over the Indian subcontinent and its surrounding oceans. The major features in the oceans as discussed earlier are distinctly visible. A few prominent

geological features in India could also be demarcated, e.g. Narmada–Son lineament, Godavari and Mahanadi rifts, Aravallis trend and the Western and Eastern ghats, etc. Also, extension of Shillong Plateau towards Andaman Block in the oceans could be demarcated. Dharwar Block and the Himalayan Plateau are also distinguishably marked in the superimposed gravity image. The major lineament trends include ENE-WSW, E-W, NE-SW,

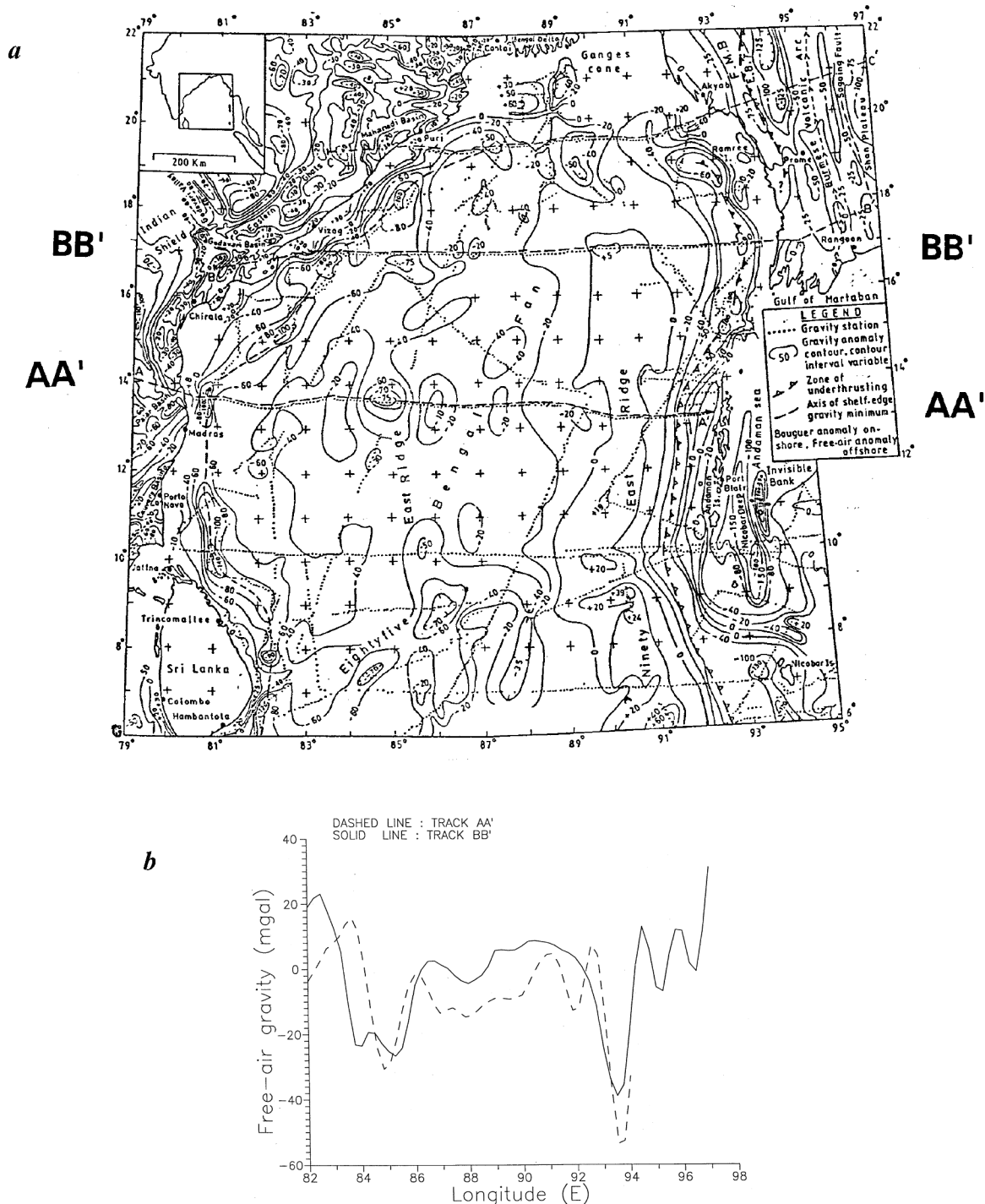


Figure 13 a, b. Comparison of ship-borne gravity with ERS altimeter-derived gravity along certain profiles in the Bay of Bengal.

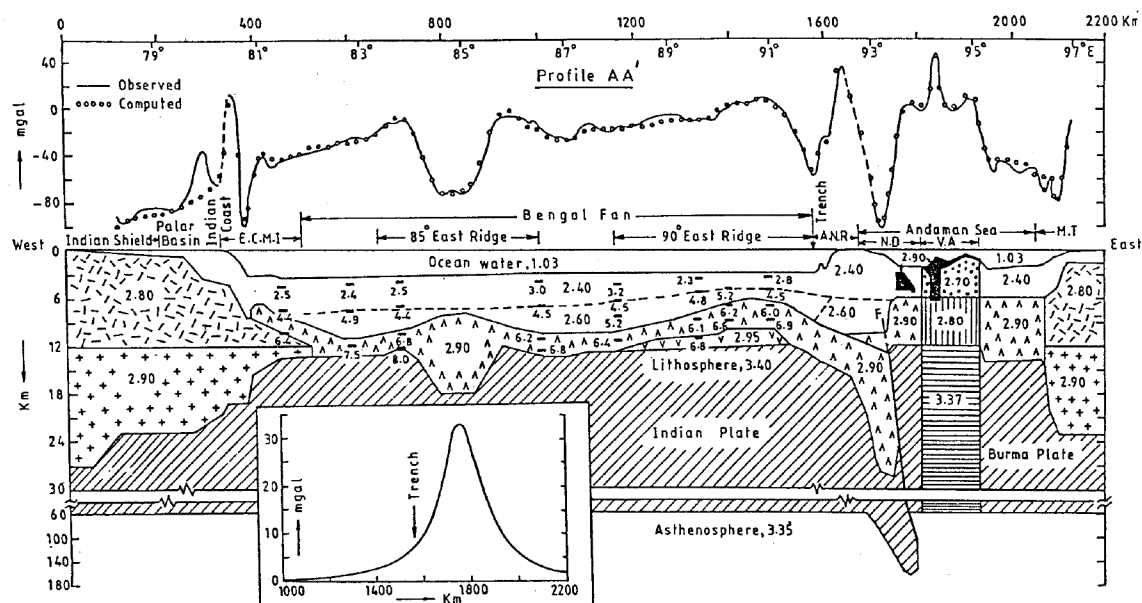


Figure 13 c. Gravity profile AA' (location, Figure 13 a, between the Indian and Malayan continental margins and its interpretation in terms of crustal and deeper lithospheric mass anomalies on the passive continental margins of India and Malaya, separated by the Andaman subduction zone. The underthrusting Indian plate below the latter acts as a zone of mass excess whose maximum gravity effect is about 32 mGal (see inset); this appears to be compensated by a low density zone under the volcanic arc. Seismic velocity information with respect to depth (as indicated by the values next to the short bars) and the sediment isopach map as given by Curray *et al.*²⁵ are used as constraints for the gravity interpretation. Larger size numbers refer to the assumed density values discussed in text. ECMI, Eastern continental margin of India; ANR, Andaman–Nicobar sediment ridge forming the Andaman–Nicobar Islands; ND, Nicobar deep; VA, Volcanic arc in the Andaman Sea; MT, Mergui Terrace. Black areas in the gravity model indicate volcanics with an inferred density of 2.90 g/cm³, F, inferred fault. After Mukhopadhyay and Krishna³².

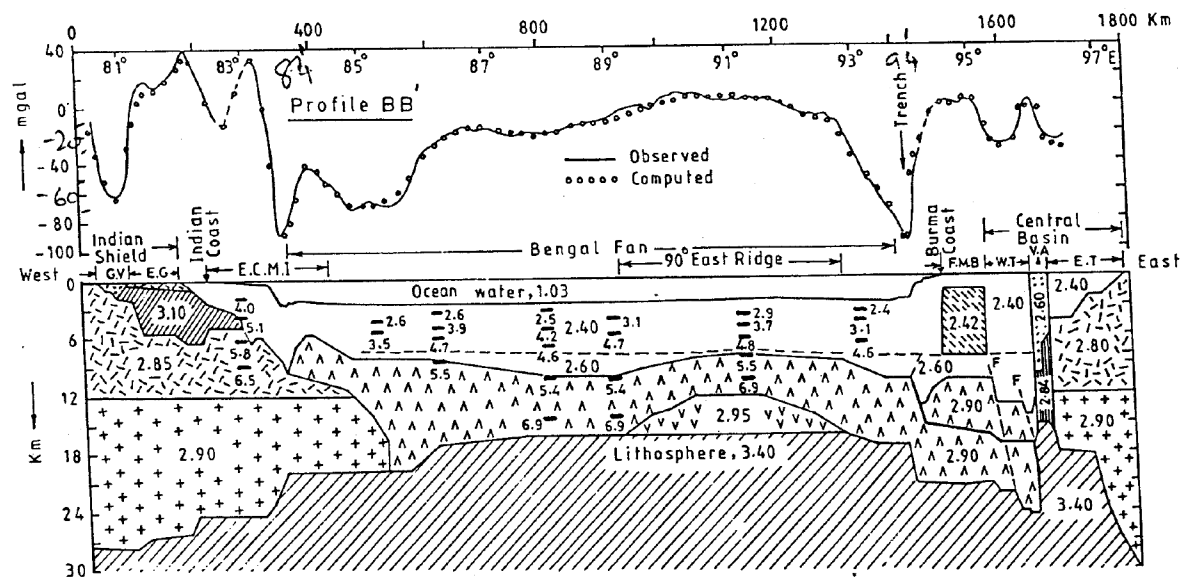


Figure 13 d. Gravity profile BB' (location Figure 13 a) and its interpretation in terms of crustal mass anomalies. All notations are the same as in Figure 7. At its eastern end the profile traverses south Burma, where the Indian plate has a fossil boundary against the Burma plate. An alternative interpretation is that subduction of the Indian plate is occurring aiseismically, but this is not supported by the gravity model. Note that the gravity model predicts: (1) Maximum sediment thickness off the Burmese coast where a relatively dense accretionary wedge (shown by oblique dashes) is inferred; (2) a compensatory mass at the crustal base to support the excess mass of the 90° East ridge (that acts as a positive subsurface load on the lithosphere); and (3) a thicker oceanic crustal wedge underlying the ECMI and its adjacent abyssal plains. GV, Godavari valley; EG, Eastern ghats; FMB, Fold mountain belt in Burma; WT and ET, Western and Eastern troughs in Burma, respectively. After Mukhopadhyay and Krishna³².

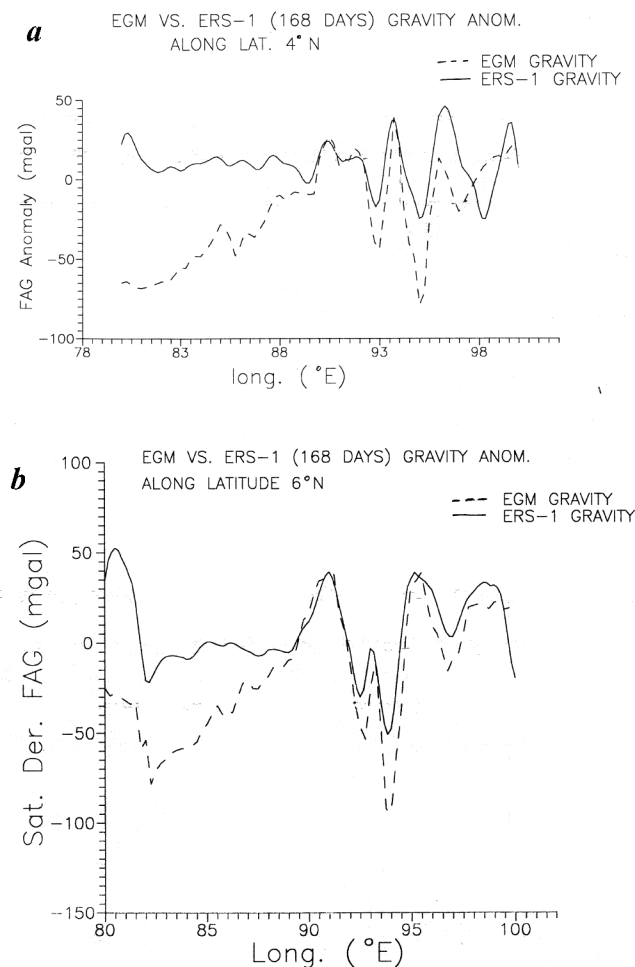


Figure 14. Comparison of free-air gravity profiles as obtained from ERS altimeter along certain fixed latitudes ((a), 4°N and (b), 6°N) in the Bay of Bengal with the profile obtained from EGM96 data.

NW-SE over land and E-W, N-S, NE-SW and NW-SE gravity linears over the Bay of Bengal and the Arabian Sea^{2,6}. Comparison of the gravity image (Figure 11) with physiography of the Indian Ocean and its surrounding land mass as obtained by Heezen and Tharp³⁰ and Lerch *et al.*³¹ using ship-borne data and ground measurements, shows conformity of the major geological features.

Figure 12 shows the EGM96 gravity over the Indian ocean and Figure 6 shows the ERS-1 altimeter-derived gravity with 35/168-day repeat data as obtained by the authors using the Satellite Gravity Method. An overall resemblance in features and trend could be observed between the two figures, which shows the efficacy of the method adopted by the authors, as EGM96 gravity has been obtained using a more rigorous method which includes theoretical modelling using spherical harmonics expansion with coefficients as high as 256, terrestrial data over land/oceans, and utilization of a number of sophisticated satellite altimeter/other related data¹⁵.

Comparison of satellite-derived gravity with ship-borne data along few profiles in the Bengal Fan region where subsurface information is available³², is shown in Figure 13 a–d. Also, comparison of satellite-derived gravity with EGM96 gravity along few profiles over the Bay of Bengal along certain fixed latitudes (4°N and 6°N) is shown in Figure 14 a and b. In both the cases, satisfactory matching could be obtained.

From the above study, the following conclusions could be made: (i) A joint gravity map over the Indian peninsula and its surrounding oceans is extremely useful for understanding the different geological processes this region has undergone since its inception to the present age, present tectonic status of this region—study of the different plate motions and their interactions, extension of certain geological features/faults from land to ocean, study of the major geological processes over land—particularly over the Himalayas, and study of the different sedimentary basins in land/ocean and the mineralogic provinces for further exploration. (ii) The major features observed in the land include Dharwar craton and southern granulite terrain, Vindhyan and Gondwana basins. Few prominent geological features in India could also be demarcated, e.g. Narmada-Son lineament, Godavari and Mahanadi rifts, Aravallis trend and the Western and Eastern Ghats, with gravity highs. A gravity high also extends in the NE direction towards lower Himalayas. Gravity lows are associated with Cuddapah basin, and Vindhyan. (iii) Satellite altimetry is an inexpensive and rapid reconnaissance tool for the sparsely surveyed Indian Ocean region. The known megastructures in both eastern and western offshore regions have been successfully demarcated using altimeter-derived geoid and gravity anomaly maps, as well as for understanding the broad tectonic setting of Indian offshore region. (iv) Gravity anomaly contour maps indicate the presence of a number of highs and lows in the area of study. The Ninety East ridge is observed as high in gravity as well as in the residual geoidal maps. Prominent gravity lows were observed in the Bengal Fan area, while the Andaman trench complex appears as a prominent high which may be due to the presence of high density rocks and its topographical anomaly. Bombay structural high is observed as a low in satellite-derived gravity as well as in ship-borne gravity. A chain of lows were observed near east coast of India, corresponding to offshore extension of five major east coast basins. (v) E-W, N-S, NE-SW and NW-SE gravity linears are prominent in the entire Bay of Bengal and east continental margin of India. Also, continental margin boundaries could be demarcated clearly in western and eastern offshore using satellite-derived gravity anomaly maps. A number of gravity linears were inferred from high gradient gravity contours which represent deep-seated faults or the sharp changes in the density variation in the area. Prominent trends are in E-W, N-S, NE-

SW, NW-SE and ENE-WSW in the Arabian Sea and the Bay of Bengal. (vi) A number of geological megastructures, e.g. Bombay High, Saurashtra platform, Ratnagiri basin, Allepy platform, Laccadive ridge, etc. in the western offshore and Cauvery basin, Krishna–Godavari basin, 90° East ridge near the Andamans in the eastern offshore have been demarcated using altimeter-derived anomaly maps. (vii) Gravity low west of margin fault zone appears to hold good amount of sediments and should be considered for further exploratory efforts in deep sea exploration. Sedimentary thickness within low west of margin fault is of the order of 2500 m, which slowly thins down to 800 m. These areas are good for exploration of gas hydrates. (viii) Comparison of results for free-air gravity as obtained by satellite-derived gravity (over oceans) and NGRI ground-based gravity (over land) with EGM96 shows good conformity as far as the trends are concerned. Also, few gravity values are matching well along certain profiles in deep oceans. Continuation of gravity patterns in land–sea crossings is yet to be investigated further, though, in a few cases, satisfactory matching could be obtained. Continuation of tectonic patterns in the land–sea crossing, e.g. extension of Owen Fracture Zone Murray ridge in the Indian and Arabian plates, and extension of 85° and 90° East ridge in the Bangladesh region through the Bengal Fan area in the eastern offshore, could be demarcated in the merged gravity image.

1. Nerem, R. S., Jekeli, C., Koblenz, J. and Beckley, B. D., *J. Geophys. Res.*, 1994, **99**, 24565–24583.
2. Ram Babu, H. V., *Curr. Sci.*, 1999, **76**, 1533–1535.
3. Biswas, S. K., *Am. Assoc. Petrol. Geol. Bull.*, 1982, **66**, 1497–1513.
4. Lundgren, B. and Nordin, P., 6th Thematic Conference, Colorado, Environmental Research Institute of Michigan, Ann Arbor, Michigan, USA, 1988, pp. 565–575.
5. Majumdar, T. J., Mohanty, K. K. and Srivastava, A. K., Joint ISRO-ONGC Report No. SAC/RSAG/TR-01/98, 1998, p. 40.
6. Majumdar, T. J., Mohanty, K. K. and Srivastava, A. K., *Int. J. Remote Sensing*, 1998, **19**, 1953–1968.
7. Mohanty, K. K. and Majumdar, T. J., *Comput. Geosci.*, 1994, **20**, 839–848.
8. Brennecke, J. and Lelgemann, D., in *Satellite Microwave Remote Sensing* (ed. Allan, T. D.), John Wiley & Sons, 1983, pp. 403–417.
9. Haxby, F., Karner, G. D., La Brecque, J. L. and Weissel, J. K., *EOS Trans. Am. Geophys. Union*, 1983, **64**, 995–1004.
10. Rapp, R. H., *J. Geophys. Res.*, 1983, **88**, 1552–1562.
11. Craig, C. H. and Sandwell, D. T., *J. Geophys. Res.*, 1988, **93**, 10408–10420.
12. McKenzie, D. and Bowin, C., *J. Geophys. Res.*, 1976, **81**, 1903–1915.
13. Srivastava, A. K., Mitra, D. S., Agarwal, R. P., Majumdar, T. J., Mohanty, K. K. and Sahai, B., ISRO-ONGC Joint Report, ONGC, Dehra Dun, 1993, p. 38.
14. NGRI Map Series, *Gravity Map Series of India* (1:5 million), National Geophysical Research Institute, Hyderabad, 1978, 1st edn.
15. Lemoine, F. G. *et al.*, NASA/GSFC Publication No. NASA/TP-1998-206861, 1998, July 1998.
16. *ERS-1 Altimeter Data User Handbook*, ESA Publication Division, France, 1993, p. 140.
17. Majumdar, T. J., Mohanty, K. K., Sahai, B., Srivastava, A. K., Mitra, D. S. and Agarwal, R. P., Tech. Rep. No. SAC/RSA/RSAG/MWRD/TR/01/94, SAC, Ahmedabad, December 1994, p. 72.
18. Chapman, M. E., *J. Geophys. Res.*, 1979, **84**, 3793–3801.
19. Davis, J. C., *Statistics and Data Analysis in Geology*, John Wiley & Sons, New York, 1973, p. 550.
20. Mahadevan, T. M., *Mem. Geol. Soc. India*, 1994, **28**, 562.
21. Qureshy, M. N., Krishna Brahmam, N., Garde, S. C. and Mathur, B. K., *Geol. Soc. Am. Bull.*, 1968, **79**, 1221–1230.
22. Srivastava, A. K., Dotiwala, F., Mitra, D. S., Majumdar, T. J. and Mohanty, K. K., ISRO-ONGC Joint Report, ONGC, Dehra Dun, 1994, p. 60.
23. Srivastava, A. K., Dotiwala, F., Majumdar, T. J. and Mohanty, K. K., ISRO-ONGC Joint Report, ONGC, Dehra Dun, 1995, p. 56.
24. Mukhopadhyay, M., *Mar. Geophys. Res.*, 1988, **9**, 197–210.
25. Curran, J. R., Emmel, F. J., Moore, D. G. and Raitt, R. W., in *The Ocean Basins and Margins* (eds Nairn, A. E. M. and Stehli, F. G.), Plenum Press, New York, 1982, vol. 6, pp. 399–450.
26. Subramaniam, C. and Singh, R. N., *Indian J. Petrol. Geol.*, 1992, **1**, 161–180.
27. Kahle, H. G. and Talwani, M., *Geophysics*, 1973, **39**, 167–187.
28. Udintsev, G. B., Fisher, R. L., Kanev, V. F., Laughton, A. S., Simpson, E. S. W. and Zhiv, D. I., *Geological and Geophysical Atlas of the Indian Ocean*, Academy of Sciences of USSR, Moscow, 1975.
29. Srivastava, A. K., Majumdar, T. J. and Mohanty, K. K., ISRO-ONGC Report, 1997, vols 1 and 2.
30. Heezen, B. C. and Tharp, M., *World Ocean Floor Panorama*, Lamont Doherty Geological Observatory, New York, 1977.
31. Lerch, F. J. *et al.*, NASA Tech. Memorandum 104555, NASA-GSFC, Greenbelt, MD, USA, 1992.
32. Mukhopadhyay, M. and Krishna, M. R., *Tectonophysics*, 1991, **86**, 365–386.
33. NOAA Reprint, US Department of Commerce, USA, 1983, p. 96.
34. Fu, L. L., Chelton, D. B. and Zlotnicki, V., *Oceanography*, 1988, **1**, 4–11, 58.
35. Dixon, T. H. and Parke, M. E., *Nature*, 1983, **304**, 406–411.

ACKNOWLEDGEMENTS. We thank the Scientific Secretary, ISRO for his suggestions and keen interest regarding this publication. We also thank Shri A. K. S. Gopalan, Director, SAC and Dr H. K. Gupta, Director, NGRI for their keen interest in this study, Dr R. R. Navalgund, Dy. Director, RESA/SAC, Dr S. Nayak, Head, MWRD/RESA, Dr D. S. Mitra, Head, R. S. Lab/KDMIPE, and Shri A. K. Srivastava, Dy. S. G., R. S. Lab/KDMIPE for their help at various stages.

Received 3 May 2000; accepted 4 November 2000